Composites Part B 243 (2022) 110139

Contents lists available at ScienceDirect

Composites Part B

journal homepage: www.elsevier.com/locate/composites

Developing aligned discontinuous flax fibre composites: Sustainable matrix selection and repair performance of vitrimers

Ali Kandemir *, Marco L. Longana, Ian Hamerton, Stephen J. Eichhorn

Bristol Composites Institute, Department of Aerospace Engineering, School of Civil, Aerospace, and Mechanical Engineering, University of Bristol, Queen's Building, University Walk, Bristol, BS8 1TR, UK

ARTICLE INFO

Keywords:
Discontinuous reinforcement
Fibre/matrix bond
Mechanical testing
Micromechanics

ABSTRACT

Sustainability of fibre reinforced polymer composites has become vital for reaching the global sustainable development goals. Natural fibres, particularly flax, and bioderived matrices are possible sustainable solutions for the composites industry, due to the constituents' embedded environmental impact reduction. According to the circular economy paradigm, sustainability can also be achieved by delaying the disposal of materials. This work reports the interfacial properties of flax fibres with three potentially sustainable advanced matrices, i.e., a vitrimer that combines the beneficial properties of both thermosets and thermoplastics, an entirely bio-based thermoset, and an advanced thermoplastic resin. Each of the selected matrices offers the potential for either recyclability, repairability, reusability, or the use of renewable sources and a reduction in the emissions of volatile organic compounds. Microbond tests were used to evaluate the interfacial shear strength and critical fibre length. It was found that the vitrimer and the bio-based thermoset matrices had a higher level of adhesion with flax fibres (~20 and ~24 MPa, respectively) compared to a traditional epoxy matrix (~12 MPa); the advanced thermoplastic resin (~6 MPa) shows the poorest adhesion. The vitrimer matrix was selected as a candidate for a sustainable and repairable discontinuous flax fibre reinforced composite. Mechanical and low-temperature rapid repair performance of an aligned discontinuous flax fibre composite, produced using the HiPerDiF method, were investigated. End-to-end and single patch repair methods were performed: vitrimer matrix composites show the potential for a mechanical strength recovery (~%50-70) that would allow them to be reused over several life cycles, enabling a circular economy.

1. Introduction

Given their high specific stiffness and strength, fibre reinforced polymer (FRP) matrix composites are a vital class of engineering materials allowing the manufacturing of light and strong structures [1–4]. Aligned discontinuous FRP (ADFRP) composites are one of the most important categories of these materials, offering good processability, *i.e.*, the capability to be formed into complex shapes with limited defects [5]. They also offer mechanical performance similar to those of continuous FRP if high levels of alignment and optimum critical fibre length are attained [6,7]. Moreover, the production of continuous FRP structures is labour intensive and produces a significant amount of manufacturing waste, which leads to high environmental impact and costs [8–10]. In contrast, manufacturing with ADFRP is potentially more sustainable as the discontinuities in the reinforcement improve their formability, facilitating defect-free manufacturing of structural parts [7,11].

The HiPerDiF method, invented at the University of Bristol [12], is a promising technology for the sustainable production of ADFRCs [13] and the remanufacturing of reclaimed carbon fibres [14]. It has been shown that ADFRPs produced *via* the HiPerDiF method have high levels of alignment [15] and their mechanical performance are similar to those of continuous FRP analogues [13]. Moreover, the HiPerDiF method provides a lower environmental impact on FRP production since the method operates with water as the alignment medium, unlike traditional glycerol methods [16,17]. Therefore, a sustainable route for high performance FRP can be potentially obtained when renewable, biodegradable, or low environmental impact composite constituents are used, such as natural fibres and sustainable matrices [18]. It has been demonstrated that natural fibres can be used without any significant deleterious effects within the HiPerDiF method despite the use of water [19]. Several natural fibres have been analysed for the HiPerDiF method [20], and their mechanical performance has been investigated [21]. These studies found that flax fibres were the best candidates amongst many natural fibres, given their higher mechanical properties and enhanced compatibility with the process.

* Corresponding author.
E-mail address: ali.kandemir@bristol.ac.uk (A. Kandemir).

https://doi.org/10.1016/j.compositesb.2022.110139
Received 1 June 2022; Received in revised form 4 July 2022; Accepted 17 July 2022
Available online 20 July 2022

To achieve high mechanical performances in ADFRP, one of the crucial parameters is the critical fibre length, which is highly dependent on the interfacial bonding between a matrix and a fibre [22]. Following the fibre selection, the fibre-matrix interface is an essential selection criterion for the sustainable matrix to develop a high-performance ADFRP. Interfacial shear strength (IFSS) is a measure of the bonding, adhesion, or the interaction between a fibre and a matrix material. By using values of the IFSS, the critical fibre length, where the fibre acts as effective reinforcement, can be calculated. The most common methods to obtain IFSS for flax fibres with different matrix systems are fibre pull-out [23–26], fibre fragmentation [27–30] and microbond tests [20,31,32].

In this study, the interfacial properties of flax fibre/sustainable matrices for high-performance ADFRPs were examined. The interfacial performance of flax fibres was investigated using the microbond test method [33] when coupled with three potentially sustainable advanced matrices:

- an advanced thermoplastic resin, which offers recyclability and reformability,
- an entirely bio-based thermoset, which offers the use of renewable sources and a reduction in volatile organic compounds (VOC) emissions,
- a vitrimer, a new class of polymer materials that shows reversible chemical cross-links and combines the beneficial properties of both thermosets and thermoplastics [34,35]; offering recyclability, repairability and reusability.

For sustainable ADFRPs, vitrimers outweigh other matrices, due to their remarkable potential for use in the circular economy [36]. It is also possible to derive them entirely from renewable sources [37]. It has been shown that a glass fibre reinforced vitrimer can be repaired by applying heat and pressure due to exchangeable disulphide crosslinks [38]. It has also been demonstrated that composite specimens can be reshaped in a hot press machine and can be recycled *via* mechanical or chemical recycling methods. Furthermore, Tanyton et al. [39] have reported an energy-neutral closed-loop recycling process for a malleable polyimine networked vitrimer resin/carbon fibre composite in which it was possible to completely recover and reuse both components. In addition, it was shown that delamination damage on carbon fibre reinforced vitrimer can be perfectly repaired through simple heat-pressing. Therefore, a vitrimer was selected as a sustainable matrix for flax fibre reinforced composites since it satisfies the principles of a zero waste hierarchy [40]. Aligned flax fibre reinforced vitrimer (ADFFRV) specimens were produced using the HiPerDiF method and investigated mechanically and physically. Two strategies were applied to repair ADFFRV, and the mechanical recovery performances were reported for the ADDFRV and vitrimer specimens.

2. Sustainable matrix selection

This part of the paper presents the interfacial characterisation and analysis of flax fibres with three potentially sustainable advanced matrices; an advanced thermoplastic, a bio-based thermoset, and a vitrimer. A promising matrix is selected for flax composites by considering the interfacial shear strengths and its possible contribution to the sustainability of FRPs.

2.1. Materials

The flax fibres were grown and processed by Eco-Technilin-Flaxtape™(Normandy, France) using a proprietary approach and were used as received. The tensile strength and diameter of the flax fibres were reported in a previous study [20], they were namely ~580 MPa and ~64 μm, respectively.

Arkema Elium®150 was selected as the advanced thermoplastic resin due to its properties such as post-thermoformability, recyclability, and mechanical properties similar to epoxy [41]. To prepare the material, a blend of resin and hardener, was mixed well manually with a 100:2 ratio, heated in an air oven at 40 °C for 20 min, and then held at room temperature overnight.

Furacure, a poly(furfural alcohol)(PFA)-based developmental resin, provided from Bitrez Ltd., was chosen as a bio-based resin, being a REACH compliant polymer [42], of high bio-based grade with fire resistance, which is advantageous in natural fibre composites [43]. The resin was prepared using a 24:1 resin to hardener ratio, manually well mixed, and cured at 160 °C for 120 min in an air oven according to recommendations by the manufacturer.

Vitrimax T100™, an imine-linked vitrimer procured from Mallinda Inc., was selected as a dynamically exchangeable covalent polymer network, offering both thermoplastic and thermoset features. Commercial vitrimers are comparative newcomers to the field of matrix chemistry, although the concept was first observed in a laboratory scale over a decade ago [44]. Vitrimax resins offer remouldability, reshaping, covalent welding, recyclability, reusability, and high mechanical performance [45,46]. To prepare the resin blend, the hardener and resin were blended in the ratio (2.5:1), then carefully mixed manually, and cured in an air circulating oven at 135 °C for 60 min.

2.2. Microbond test

The microbond method [33] was applied to determine the interfacial shear strength (IFSS) of flax fibres with each of the selected matrices. A schematic and a picture of the experimental test setups for the microbond tests are shown in Fig. 1. The fibres were mounted between plastic end-tabs arranged in a silicone holder to maintain a gauge length of 40 mm. Dynamax 3139 adhesive was used to bond the fibres to the end-tabs, and this was cured at ambient temperature (~20 °C) under UV light (λ = 368 nm) for at least 2 h. Resin droplets were then applied to the fibres and cured following the procedures outlined in Section 2.1. An optical microscope, Zeiss Axio Imager M2 (Carl Zeiss AG, Oberkochen, Germany), was used to measure the droplet position on the fibre, its size, and the embedded area for each microbond test specimen. For the microbond test, a Dia-stron LEX820 Extensometer (Dia-Stron Ltd., Andover, UK) was used to deform the samples with a microbond apparatus, which comprises of a microvice, *i.e.*, a thin metallic plate with a narrow cut in the middle to accommodate the fibre but to prevent the microdroplet from passing through (see Supporting Information Fig. 1S). Microvice gap separation was varied (gap sizes; 50, 80, 150, and 180 μm) depending on the diameter of the droplet, which ranged from ~70 up to 1000 μm, to achieve an ideal contact for force distribution. More than 150 droplets were prepared for each matrix system. However, the number of droplets produced and successfully tested for each flax/matrix combination were 62, 57, 66, and 73 for Elium, epoxy, Furacure, and Vitrimax resins, respectively. Moreover, droplet embedded length varied between 260–1200, 180–900, 150–650, and 170–1300 μm for Elium, epoxy, Furacure, and Vitrimax, respectively. After each test, the fibre was observed using an optical microscope to determine if debonding had occurred. Specimens that showed debonding failure mechanisms were deemed admissible for the calculation of IFSS. The IFSS between fibre and matrix was calculated using Eq. (1):

$$\tau = \frac{F_d}{\pi d l_e} \tag{1}$$

where τ, F_d, d, and l_e denote IFSS, debonding force, fibre diameter and embedded length, respectively. In Eq. (1), the denominator represents the embedded area. It is worth mentioning that the high surface roughness of flax fibres, 10 times higher than glass fibres [20], and their elliptical cross-section [20] may have an effect on the calculated IFSS value. However, to a first approximation, a circular cross section was

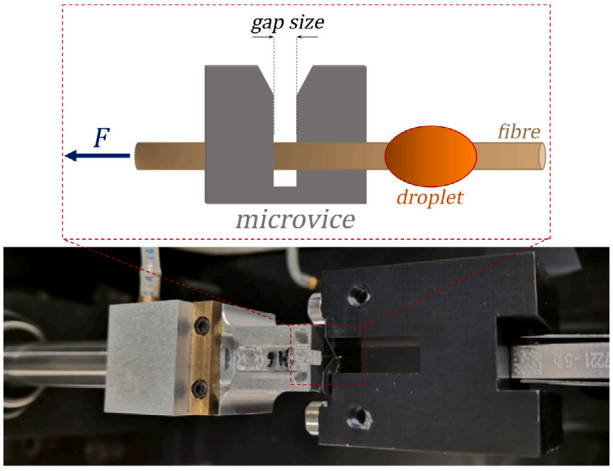

Fig. 1. A schematic setup of the microbond test (above) and a photograph of the experimental setup (below).

assumed since only a single fibre type is studied here for comparison purposes.

For efficient reinforcement in short or discontinuous fibre reinforced composites, the filaments must have lengths exceeding the critical fibre length. This then maximises stress transfer between the constituents, and the failure of the composite material is likely to be initiated by the fibres rather than fibre-matrix debonding. The critical fibre length is calculated using the following Eq. (2):

$$l_c = \frac{d\sigma_f}{2\tau} \tag{2}$$

where l_c, d, and σ_f represent the critical fibre length, diameter (within the droplet), and fibre tensile strength, respectively.

2.3. Results and discussion

Fig. 2 shows the microbond test results for the sustainable matrices coupled with flax fibre as a function of force and embedded area. As reported before, fibres, exhibit several failure mechanisms during a microbond test. These include shear failure (debonding), fibrillation of fibres within the droplet (fibrillation), fibre failure in the vicinity of the droplet (FFD), fibre failure (FF), and broken matrix (BM); a summary of these has been previously published by Kandemir et al. [20]. Examples of debonding failure, the mechanism experimentally admissible for the calculation of IFSS, from the performed microbond tests for all samples are shown in Supporting Information (see Fig. S1–S3). To better understand the interfacial performance of potential sustainable resins, flax-epoxy (PRIME™20LV) system data from a previous study [20], which was obtained with the same experimental methodology, were included in this study for comparison.

A linear fit that passes through the origin was applied to the debonding data to get the IFSS value, τ_{fit}, for the investigated fibre/resin combinations. τ_{fit} and τ_{mean}, which is the average IFSS values calculated for each debonding data using Eq. (1), are given in Table 1. A good consistency was found between τ_{fit} and τ_{mean}. Moreover, τ_{fit} lines were in good agreement by being within the range of upper and lower bounds of 95% confidence intervals, as highlighted in Fig. 2.

Different behaviours were observed in failure types of flax fibres with the advanced matrices. Fibre failures (FF and FFD) are less frequently observed for Elium and epoxy matrices as compared to Furacure and Vitrimax matrices. These data indicate that matrices with stronger IFSS tend to show more fibre failure when coupled with natural fibres. It is noted also that fibrillation failure occurs before the applied force reaches the point of debonding, indicating that the fibres have weaker interactions between the fibrils than the bond with the resin. Moreover, a BM type failure was observed for small embedded areas (up to 0.10 mm^2) for thermoset based matrices, whereas the thermoplastic-based matrix (Elium) exhibited the same failure type to 0.25 mm^2. This may imply that BM type failure is expected for smaller thermoset droplets in which the microvice damages the matrix, or for thermoplastic droplets where there is an insufficient degree of bonding within the microdroplet (see Fig. S4, Supporting Information). Moreover, the residual stresses developed during the specimen manufacturing stage, caused by the different curing or heat treatment required by each polymer, may influence the results of the microbond test; however, their effect is intrinsic to a particular fibre polymer combination.

Table 1
Interfacial shear strength values obtained by linear fitting (τ_{fit}) and the mean of interfacial shear strength values (τ_{mean}), critical fibre length (l_c), and critical aspect ratio (AR_c) of Elium, epoxy, Furacure and Vitrimax matrices coupled with flax fibres. ρ and errors, ±, represent the correlation coefficient, and standard errors of the mean, respectively.

Flax Fibre coupled with	τ_{fit} (MPa)	τ_{mean} (MPa)	l_c (mm)	AR_c (mm/mm)
Elium	5.9 (ρ:0.96)	5.9 ± 0.2	3.1 ± 0.7	48.9 ± 6.6
Epoxy	11.4 (ρ:0.77)	11.8 ± 0.8	1.6 ± 0.4	24.4 ± 4.2
Furacure	23.1 (ρ:0.90)	23.7 ± 1.5	0.8 ± 0.2	12.2 ± 2.1
Vitrimax	18.3 (ρ:0.78)	20.0 ± 1.5	0.9 ± 0.2	14.5 ± 2.6

To compare IFSS values of the microbond test data, statistical analysis was carried out using analysis of variance evaluated at a 95% level of significance and a p-value <0.05. Fig. 3 presents this analysis, showing the variance of IFSS values of Elium, epoxy, Furacure and Vitrimax matrices with flax fibres.

This analysis demonstrates that Elium has a significantly lower IFSS than epoxy resin. In addition, these are both significantly different to Furacure and Vitrimax, which were found to have no statistically significant difference. It was found that Elium shows the lowest adhesion performance with flax fibres. On the other hand, the Furacure and Vitrimax resins showed the highest level of adhesion, and they have a higher level of adhesion with flax fibres than the standard Prime20LV epoxy system. Moreover, the IFSS values for flax with different epoxy systems have been reported variously as 13–17 MPa [26], 23 MPa [47] by pull-out tests, 16–24 MPa (Prime20LV system) [29] by single yarn fragmentation test, and 33 MPa (24 MPa with maleic anhydride sizing) [30] by using single fibre fragmentation tests. It is noted here that the 'round-robin' test programme has also shown that pull-out tests give a higher IFSS value than the microbond tests [48]. Therefore, Furacure and Vitrimax are expected to have a higher IFSS, given that pull-out or fibre fragmentation tests have typically been carried out on these resin systems. Although there is no consensus on which tests are the most reliable, it is expected that the IFSS values of both resin systems will be noticeably higher than the reported values in this study, hence also reflecting higher tensile strength values for FRPs [49].

Fig. 4 reports both the critical fibre length and the critical aspect ratio (AR_c) values of the all matrix — flax fibre systems. The data are also summarised in Table 1. Increased reinforcement in discontinuous flax FRP can be obtained when fibres with longer lengths than the reported critical length values are used in the manufacturing stages. Moreover, the critical aspect ratio concept may be of more technical relevance than the critical fibre length [50], because different manufacturing processes may deliver fibres with different diameters but similar mechanical properties [51].

2.4. Sustainable matrix selection

In the first part of this paper, the interfacial properties of flax fibres with three potentially sustainable advanced matrices were investigated and were compared with a commonly used commercial epoxy. It was found that Furacure and Vitrimax matrices are good candidates for

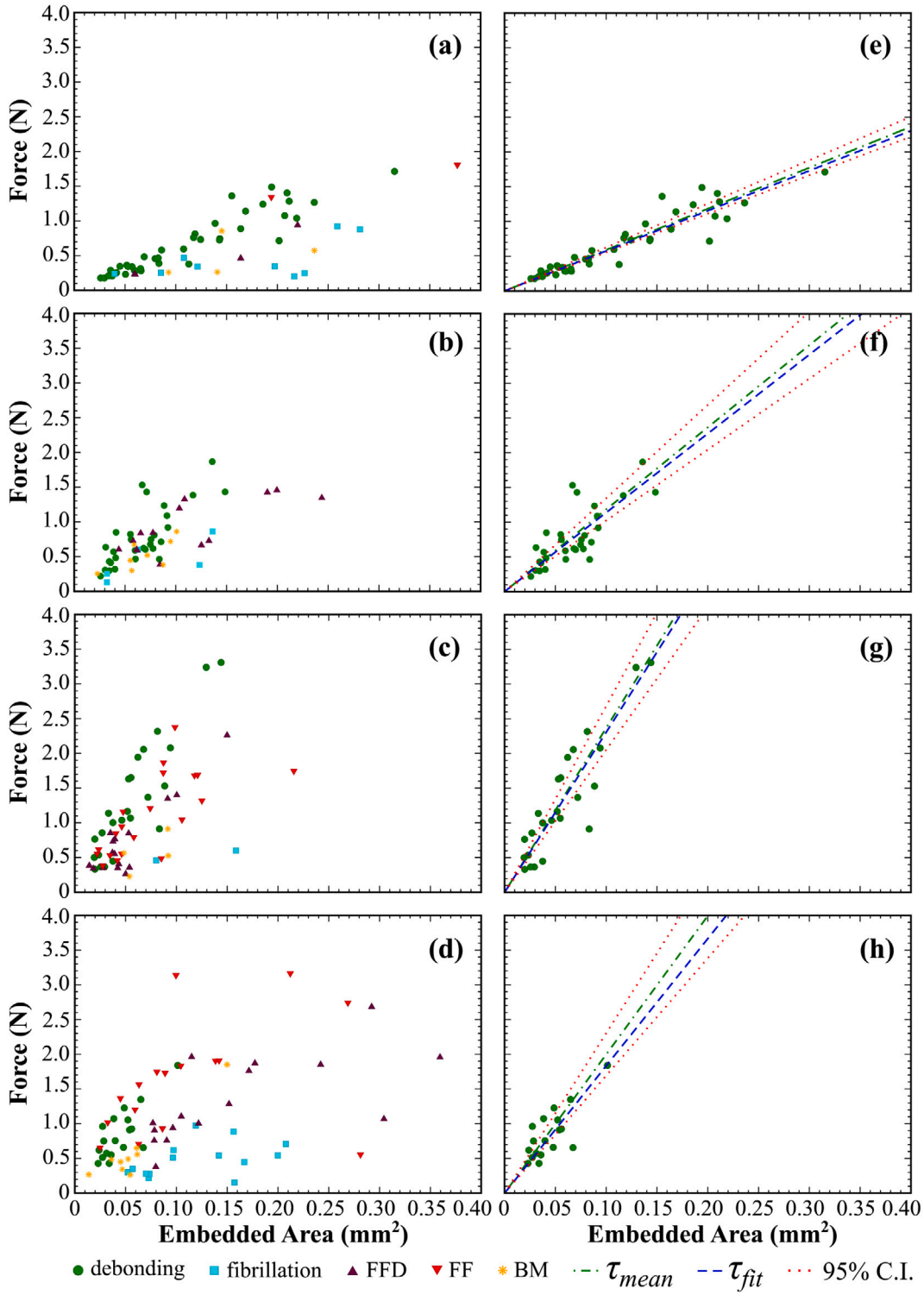

Fig. 2. Microbond test results of flax fibres with the (a,e) Elium, (b,f) epoxy, (c,g) Furacure, and (d,h) Vitrimax matrices in terms of force versus embedded area. (a–d) shows all data obtained from the test consisting of different failure mechanisms, (e–h) panel shows data only for debonding failure (green dots). Green dash-dotted and blue dashed lines represent τ_{mean} and τ_{fit}, respectively. Red dotted lines show the upper and lower 95% confidence intervals (C.I.). (For interpretation of the references to colour in this figure legend, the reader is referred to the web version of this article.)

making sustainable composites with flax fibres thanks to high interfacial shear strength. Since reuse, repair, and recycling options fit with end-of-life goals and provide more use of the already made-material, the Vitrimax matrix was selected for further mechanical and physical examination within discontinuous flax fibre composites.

3. Repair performance of vitrimer

This part of the paper presents the manufacturing, mechanical and physical characterisation of short flax fibre reinforced vitrimers. In addition, the rapid low-temperature repair performance of aligned discontinuous flax fibre reinforced vitrimers (ADFFRVs) is uncovered.

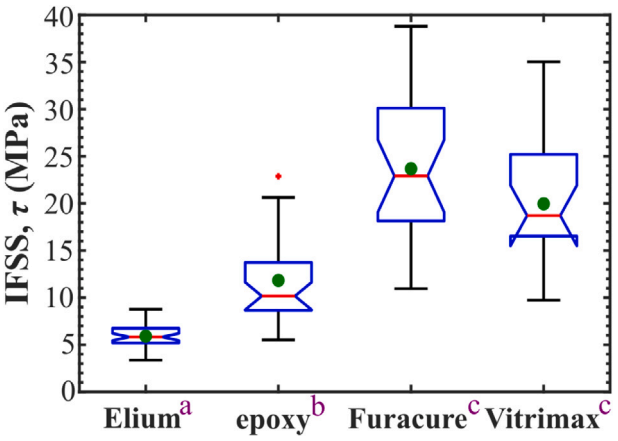

Fig. 3. Analysis of variance of interfacial shear strength data of Elium, epoxy, Furacure and Vitrimax matrices with flax fibres. Green dot, red line, black lines, and blue lines show mean, median, maximum and minimum values, and quarter percentiles and control limit values, respectively. Unique letters a, b, and c represent where there is a statistical difference ($p < 0.05$, N = 132), or not (c, $p > 0.05$), for resins. (For interpretation of the references to colour in this figure legend, the reader is referred to the web version of this article.)

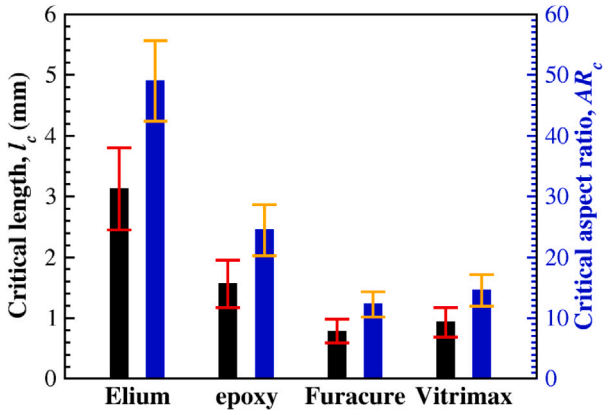

Fig. 4. The critical fibre lengths, l_c (black), and the critical aspect ratio values, AR_c (blue) of Elium, Furacure and Vitrimax with flax fibres. Error bars represent the standard errors of the mean.

3.1. Materials and manufacture

To manufacture composite specimens, four layers of aligned 6-mm long flax fibre preforms (75–85 gsm) produced *via* the water based HiPerDiF fibre alignment method were sandwiched between five layers of Vitrimax T100™ resin film (150–250 gsm) sourced from Mallinda Inc. Further information about the use of the HiPerDiF technology to align natural fibres can be found in [19,21]. The composite stack was then cured by vacuum bag moulding in an autoclave at 135 °C at 1 bar pressure for 30 min followed by another 30 min at ~6.5 bar pressure. Pure vitrimer resin specimens were prepared using the same semi-closed mould and cured at 135 °C at 1 bar for 30 min followed by another 5 min at 3 bar. The glass transition temperature, T_g, of Vitrimax T100™ is 100 °C and the theoretical topology freezing temperature, T_v, has not been disclosed. Since T_v is governed by T_g in polyimine vitrimer systems, it can be assumed that T_v is lower than or equal to the T_g value and can be determined by dynamic mechanical analysis [52].

3.2. Testing methodology

3.2.1. Tensile test

Referring to ASTM D3039/D3039M-17 [53], the ADFFRV and vitrimer specimens were tensile tested on an electro-mechanical testing machine at a test speed of 1 mm min^{-1}. Extension was measured using a video extensometer (IMETRUM, Bristol, UK) and converted to strain. A 10 kN load cell (Shimadzu, Kyoto, Japan) was used to record the load. The nominal sizes for specimens' widths and lengths were 5 and 150 mm, respectively; no end-tabs were used, and the specimens were gripped with hand-screwed clamps leaving a 50 mm gauge length. The specimen thicknesses were between 1.1–1.4 mm for the ADFFRV specimens and between 0.6–0.7 mm for the vitrimer specimens.

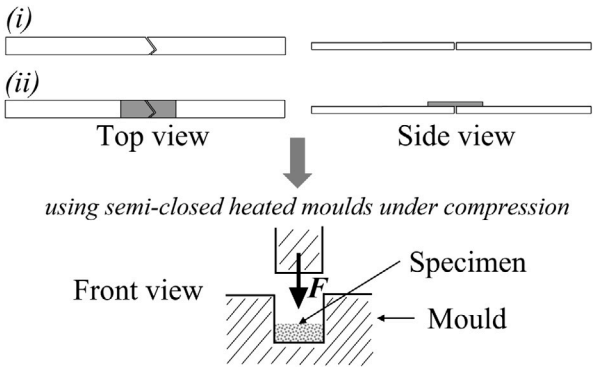

Fig. 5. Schematics of two composite repair strategies taken from a top view and a side view of the specimens; (i) end-to-end repair and (ii) single-patched on samples that are pre-fractured and repaired using (ii), and a schematic representation of the repair process. White filled shapes and grey filled rectangular regions represent the fractured specimen pieces and a patch, respectively. The patch is identical to the original specimen.

3.2.2. Visual characterisation

A high-resolution scanner (Epson Expression 11000XL, Epson, Shinjuku, Tokyo) was used to acquire high-resolution images of the fractured regions of the composite specimens. An optical microscope (Zeiss Axio Imager M2, Carl Zeiss AG, Oberkochen, Germany) was used to analyse cross-sections of the composite specimens. Cold mounting followed by standard wet grinding and polishing for polymer matrix composites was applied to make the specimens for cross-section analysis. A scanning electron microscope (Hitachi TM3030Plus, Hitachi, Ltd., Tokyo, Japan) was used to analyse the fracture surfaces of the composite specimens.

3.2.3. Repair strategy

A low-temperature and rapid technique was devised in order to assess the repair performance of aligned discontinuous flax fibre vitrimers. Broken samples were placed in a semi-closed mould that was then located between heated plates in a 50 kN load cell (Instron, Buckinghamshire, UK). Then a 0.69 MPa pressure was applied for 5 min at 120 °C to repair the samples. The broken ends of the samples were placed in contact with one another, and two repair strategies were tested; (i) unpatched and (ii) single-patched on samples that had already been broken and repaired using method (i). Methods (i), (ii), and the repair process are represented schematically in Fig. 5. Patches were obtained from a spare specimen and assumed to be identical to the original specimen in terms of fibre volume fraction and alignment. For comparison, vitrimer specimens also were repaired using method (i). However, during repair, the pressure was applied for only 3 min, again at 120 °C to prevent resin leaking at the edges of the sample and drastic dimensional changes.

3.3. Results and discussion

3.3.1. Mechanical properties of original and repaired vitrimer

Tensile tests were performed to obtain the mechanical properties of the vitrimer. In total, six pure vitrimer specimens were tested: four

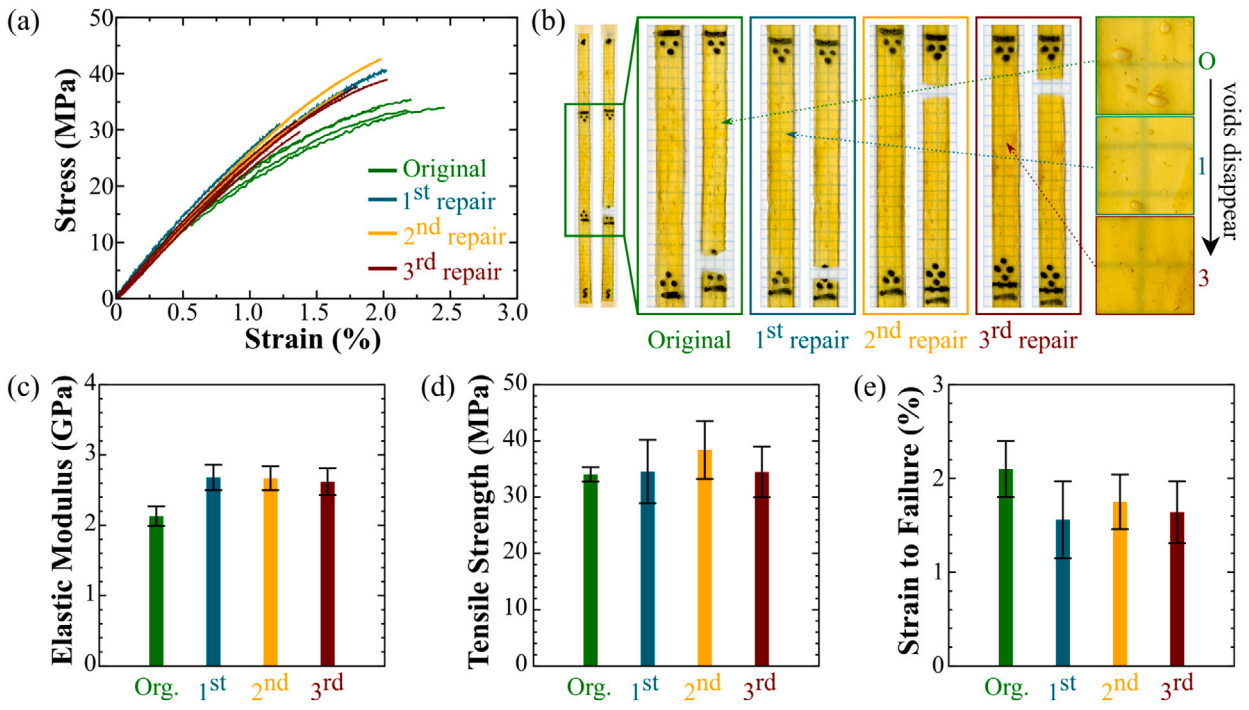

Fig. 6. (a) Representative stress–strain curves, (b) high resolution images, (c) elastic modulus, (d) tensile strength, and (e) strain to failure of the original (Org.) and repaired (1st, 2nd, 3rd repairs) vitrimer specimens. Errors represent standard deviations (SD) from the mean. (For interpretation of the references to colour in this figure legend, the reader is referred to the web version of this article.)

successfully broke within the gauge length, and were used to calculate the mechanical properties of the as-manufactured specimens. Those specimens were then repaired, once, twice, and thrice. Fig. 6 reports representative stress–strain curves, typical high-resolution images and the mechanical properties of as-manufactured (original) and repaired vitrimer specimens.

As seen in Fig. 6a, the stress–strain curves of the repaired specimens show similar trends and comparable values of failure strain and strength. There is however a noticeable difference from the original curves, where the data deviate more markedly from linearity compared to the repaired specimens. Fig. 6c, d, and e show elastic modulus, tensile strength, and strain to failure of the vitrimer specimens, respectively. In addition, the mechanical properties are summarised in Table 2. A statistically significant increase was observed in elastic modulus values from the original to a first time repaired vitrimer specimen, after which a plateau was reached for further repairs. The reason for the modulus increase was thought to be the extraction of air (see Fig. 6b) from trapped voids between the vitrimer film layers during the manufacturing process, and caused by the high-pressure applied during the first repair step in which a temperature above $T_g \sim T_v$ was applied. The failure regions of specimens were inspected and found to be far from the location where there are visible voids. No significant change was observed between the original and repaired vitrimer specimens in terms of tensile strength. Tensile strength values were found to be consistent with the stress at break of a crosslinked polyimine network, which has been reported to be ~40 MPa [46] and 10–60 MPa [39] from two independent studies. Furthermore, a slight decrease was seen for the strain to failure from the original to repaired vitrimer specimens.

3.3.2. Mechanical properties of original and repaired flax fibre reinforced vitrimers

The mechanical properties of the ADFFRVs were determined, both on original and repaired specimens. In total, six specimens were tested, of which five (four for single side patched ADFFRV) successfully broke within the gauge length and were used to calculate the mechanical properties. Fig. 7 reports representative stress–strain curves, high-resolution images, mechanical properties, and scanning electron micrographs of original, repaired, and patched ADFFRV specimens. The expected fibre volume fraction calculated using the average areal weights and densities of the constituents was found to be 17.9% (see Equation S1, Supporting Information). The mechanical properties of fractured and repaired ADFFRVs are summarised in Table 3.

Table 2
Mechanical properties of as-manufactured (original) and repaired vitrimers (VitrimaxT100). Errors represent SD from the mean.

	Elastic modulus (GPa)	Tensile strength (MPa)	Strain to failure (%)
Original	2.1 ± 0.1	34.1 ± 0.8	2.1 ± 0.3
1st repair	2.7 ± 0.2	34.5 ± 5.6	1.6 ± 0.4
2nd repair	2.7 ± 0.2	38.4 ± 5.2	1.7 ± 0.3
3rd repair	2.6 ± 0.2	34.5 ± 4.5	1.6 ± 0.3

As seen in Fig. 7a, there are decreasing trends in the stress–strain curves of the ADFFRV specimens in terms of their slope, and the strain and stress values at failure for each end-to-end repair stage. In contrast, the patched repair specimens showed a moderate increase in properties. Fig. 7c shows the elastic modulus of the ADFFRV specimens; agreement was found between the expected elastic modulus calculated using the rule of mixtures (see Equation S2, Supporting Information) and the experimentally determined values of the as-manufactured ADFFRV, 11.5 ± 0.7 GPa and 11.5 ± 0.8 GPa, respectively. In addition, a dramatic increase was seen in elastic modulus values of end-to-end repair stages. After the patched repair method, a decrease in the elastic modulus value towards the original value was observed.

Fig. 7d shows the tensile strength of the ADFFRV specimens. A good correspondence was also found between the expected tensile strength estimated using the simple rule of mixtures, which is 131.7 ± 4.9 MPa (see Equation S3, Supporting Information), and the tensile strength of the original ADFFRV, which is 121.2 ± 14.4 MPa. Moreover, it was seen that there is a negative exponential saturation trend towards

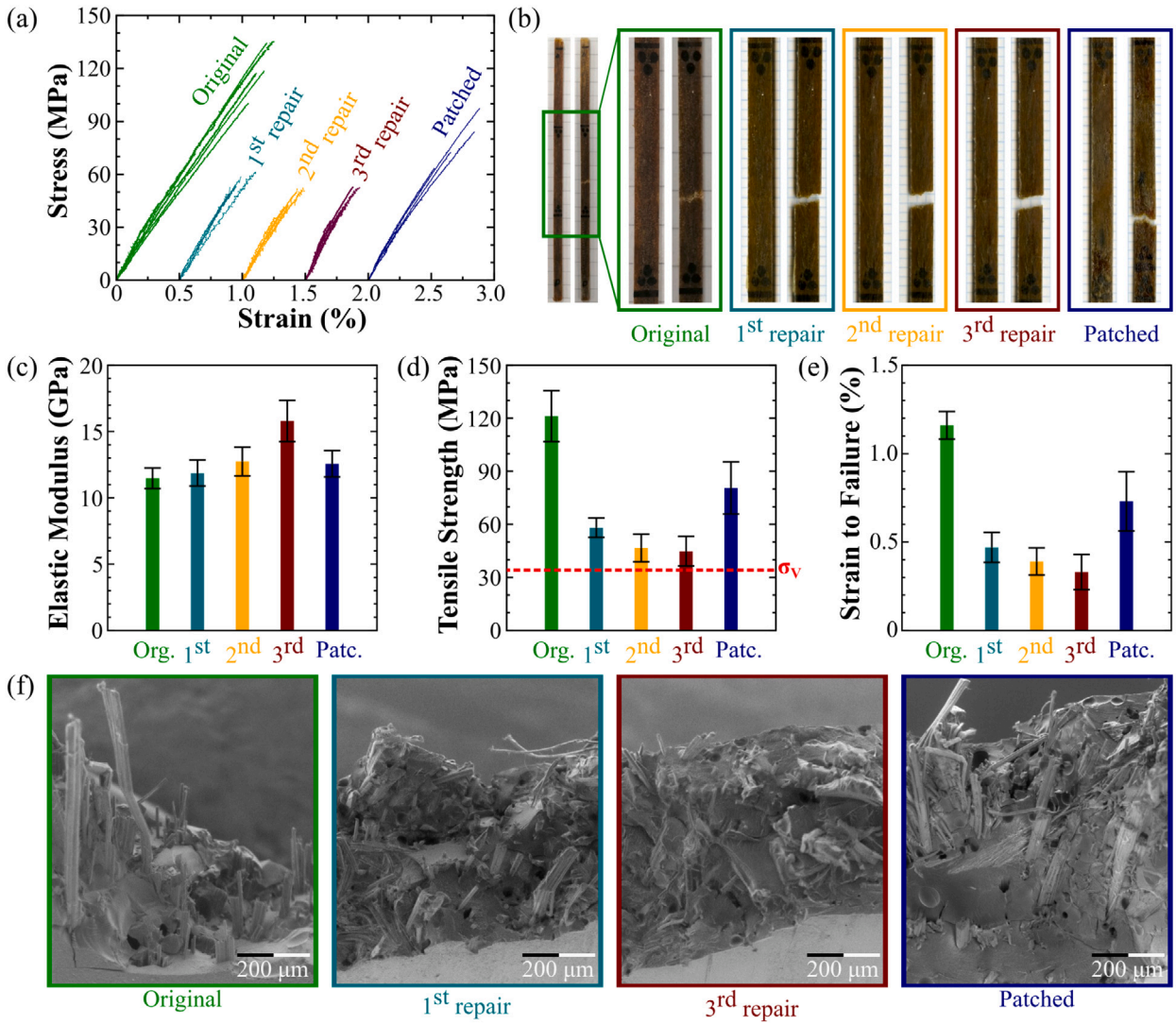

Fig. 7. (a) Representative stress–strain curves, (b) high resolution images, (c) elastic modulus, (d) tensile strength (red line represents tensile strength of the vitrimer), (e) strain to failure for original (Org.) and repaired (1st, 2nd, 3rd repairs) and patched (Patc.) specimens, (f) typical scanning electron micrographs of the original and repaired ADFFRV specimens. Errors represent SD from the mean. In (a), 0.5, 1.0, 1.5, and 2.0% strain reference points are the starting points, respectively, for the 1st, 2nd, 3rd, and patched repairs. (For interpretation of the references to colour in this figure legend, the reader is referred to the web version of this article.)

Table 3
Mechanical properties of as-manufactured (original) and repaired aligned flax fibre reinforced vitrimers. Rule of mixtures (RoM) is calculated for v_f = 17.9% and details can be found in Supporting Information. Errors represent SD from the mean.

	Elastic modulus (GPa)	Tensile strength (MPa)	Strain to failure (%)
RoM	11.5 ± 0.7	131.7 ± 4.9	–
Original	11.5 ± 0.8	121.2 ± 14.4	1.2 ± 0.1
1st repair	11.9 ± 1.0	58.1 ± 5.5	0.5 ± 0.1
2nd repair	12.7 ± 1.1	46.6 ± 7.8	0.4 ± 0.1
3rd repair	15.8 ± 1.5	44.1 ± 8.4	0.3 ± 0.1
Patched	12.6 ± 1.0	80.6 ± 14.7	0.7 ± 0.2

the tensile strength of the vitrimer in end-to-end repair cycles of ADFFRV specimens. As seen in the high resolution scans of tensile tested ADFFRV specimens (Fig. 7b), the failure points occurred in the same locations as the original materials for all the end-to-end repaired samples. Additionally, the failure regions became less rough, indicating a lower presence of fibres and a more resin dominated healing. When the patching repair method was applied to the three times repaired ADFFRV, the failure region became more jagged. In addition, the fibres became noticeable on the failure surface, which is in a slightly different location compared to the previous failures.

As seen in Table 3, an almost doubling of tensile strength was seen for the patched repaired ADFFRV samples compared to the three times repaired materials; this in turn is nearly two-thirds of the original samples. To reveal the reason behind the change in mechanical performances in repaired ADFFRV, scanning electron microscopy analysis was carried out for the failure region of ADFFRV specimens, as shown in Fig. 7f. It can be seen that there are aligned fibres in the failure region of the original ADFFRV. There are however fewer aligned or distorted fibres, and in some regions no fibres at all, in the end-to-end repaired ADFFRVs. As observed in high resolution scans of tensile tested ADFFRV, the presence and condition of fibres were changed after repair and affected the mechanical performance of the composites. After the patch repair, the number of aligned fibres increased, which explains the increase in tensile strength, and some distorted fibres were observed. In the images of the cross-sections of the patched and original specimens, no significant differences were observed (see Fig.S5–8, Supporting Information). Moreover, a significant decrease was observed for the strain to failure values in the end-to-end repair specimens. An increase in the strain to failure value towards the value

of the original composites was seen in the patched specimens after three times of repairing ADFFRV.

4. Conclusion

The interfacial properties of flax fibres with three potentially sustainable advanced matrices have been reported and compared with a commonly used commercial epoxy matrix. The bio-based (PFA) and vitrimer (imine-linked) resins were observed to be good candidates for producing sustainable composites with flax fibres due to high IFSS values. A vitrimer resin was selected as a promising candidate for sustainable discontinuous flax fibre composites, and its repair performance was examined. End-to-end and single patch repair methods were used as a repair strategy to investigate the repair capabilities of the vitrimer resin in flax fibre reinforced composites. It was found that a rapid and low-temperature end-to-end repair strategy is able to recover half of the strength of the as-manufactured composites; however, the single patch repair method showed better recovery (~67%) than end-to-end repair. In addition, the single patch repair method might show better mechanical recovery when applied as first repair strategy. Time, temperature, and pressure must be optimised to identify the maximum repair performance of fibre-reinforced vitrimer composites. In conclusion, aligned natural fibre reinforced vitrimers can be reused, repaired, and recycled: this represents a step towards a circular economy and sustainability in fibre reinforced composites applications, especially in automotive, transport, and sporting goods industries in which weight reduction, the use of renewable sources, and sustainability are essential.

CRediT authorship contribution statement

Ali Kandemir: Conceptualization, Data curation, Formal analysis, Funding acquisition, Investigation, Methodology, Visualisation, Writing – original draft, Writing – review & editing. **Marco L. Longana:** Conceptualization, Funding acquisition, Supervision, Writing – review & editing. **Ian Hamerton:** Conceptualization, Funding acquisition, Supervision, Writing – review & editing. **Stephen J. Eichhorn:** Conceptualization, Funding acquisition, Supervision, Writing – review & editing.

Declaration of competing interest

The authors declare that they have no known competing financial interests or personal relationships that could have appeared to influence the work reported in this paper.

Data availability

All underlying data are provided in this published article (and its supporting information files).

Acknowledgements

The authors thank Ecotechnilin, Fabrizio Scarpa, and Charles de Kergariou for supplying flax fibres. The authors also thank Mallinda Inc. (especially Heather Rubin) and Bitrez Ltd. (especially Dominic Hopwood) for providing polymer matrix materials. The funders had no role in the design of the study; in the collection, analyses, or interpretation of data; in the writing of the manuscript, or in the decision to publish the results.

Funding

This work was funded under the UK Engineering and Physical Sciences Research Council (EPSRC) Project [grant EP/P027393/1] "High Performance Discontinuous Fibre Composites—a sustainable route to the next generation of composites" and the EPSRC Centre for Doctoral Training at the Advance Composites Centre for Innovation and Science (ACCIS, Grant number EP/L016028/1). A.K. acknowledges support from Turkish Ministry of National Education YLSY grant.

Appendix A. Supplementary data

Supplementary material related to this article can be found online at https://doi.org/10.1016/j.compositesb.2022.110139.

References

[1] Soutis C. Fibre reinforced composites in aircraft construction. Prog Aerosp Sci 2005;41(2):143–51.
[2] Rubino F, Nisticò A, Tucci F, Carlone P. Marine application of fiber reinforced composites: a review. J Mar Sci Eng 2020;8(1):26.
[3] Mishnaevsky L, Branner K, Petersen H, Beauson J, McGugan M, Sørensen B. Materials for wind turbine blades: an overview. Materials 2017;10(11):1285.
[4] Adam H. Carbon fibre in automotive applications. Mater Des 1997;18(4):349–55.
[5] Hassan MH, Othman AR, Kamaruddin S. A review on the manufacturing defects of complex-shaped laminate in aircraft composite structures. Int J Adv Manuf Technol 2017;91(9):4081–94.
[6] Fu S-Y, Lauke B. Effects of fiber length and fiber orientation distributions on the tensile strength of short-fiber-reinforced polymers. Compos Sci Technol 1996;56(10):1179–90.
[7] Matthew Such CW, Potter K. Aligned discontinuous fibre composites: A short history. J Multifunct Compos 2014;2(3):155–68.
[8] Artetxe E, González H, Calleja A, Valdivielso AF, Polvorosa R, Lamikiz A, Lacalle LNLD. Optimised methodology for aircraft engine IBRs five-axis machining process. Int J Mechatron Manuf Syst 2016;9(4):385–401.
[9] Yao Y, Li M, Lackner M, Herfried L. A continuous fiber-reinforced additive manufacturing processing based on PET fiber and PLA. Materials 2020;13(14).
[10] Chacón J, Caminero M, Núñez P, García-Plaza E, García-Moreno I, Reverte J. Additive manufacturing of continuous fibre reinforced thermoplastic composites using fused deposition modelling: Effect of process parameters on mechanical properties. Compos Sci Technol 2019;181:107688.
[11] Ward C, Hazra K, Potter K. Development of the manufacture of complex composite panels. Int J Mater Prod Technol 2011;42(3–4):131–55.
[12] Yu H, Potter K. Method and apparatus for aligning discontinuous fibres, UK patent, Patent application (filed: 2013-04-15, application granted: 2017-07-19).
[13] Yu H, Potter K, Wisnom M. A novel manufacturing method for aligned discontinuous fibre composites (High Performance-Discontinuous Fibre method). Composites A 2014;65:175–85.
[14] Longana ML, Yu H, Jalavand M, Wisnom MR, Potter KD. Aligned discontinuous intermingled reclaimed/virgin carbon fibre composites for high performance and pseudo-ductile behaviour in interlaminated carbon-glass hybrids. Compos Sci Technol 2017;143:13–21.
[15] Longana ML, Yu H, Lee J, Pozegic TR, Huntley S, Rendall T, Potter KD, Hamerton I. Quasi-isotropic and pseudo-ductile highly aligned discontinuous fibre composites manufactured with the HiPerDiF (high performance discontinuous fibre) technology. Materials 2019;12(11).
[16] Bagg G, Evans M, Pryde A. The glycerine process for the alignment of fibres and whiskers. Composites 1969;1(2):97–100.
[17] Bagg GEG, Edwards H, Evans MEN, Lewis JA, Ziebland H. Aligning fibres. 1976, US Patent 3, 947, 535.
[18] Fitzgerald A, Proud W, Kandemir A, Murphy RJ, Jesson DA, Trask RS, Hamerton I, Longana ML. A life cycle engineering perspective on biocomposites as a solution for a sustainable recovery. Sustainability 2021;13(3):1160.
[19] Longana M, Ondra V, Yu H, Potter K, Hamerton I. Reclaimed carbon and flax fibre composites: manufacturing and mechanical properties. Recycling 2018;3(4):52.
[20] Kandemir A, Pozegic TR, Hamerton I, Eichhorn SJ, Longana ML. Characterisation of natural fibres for sustainable discontinuous fibre composite materials. Materials 2020;13(9).
[21] Kandemir A, Longana ML, Panzera TH, del Pino GG, Hamerton I, Eichhorn SJ. Natural fibres as a sustainable reinforcement constituent in aligned discontinuous polymer composites produced by the HiPerDiF method. Materials 2021;14(8):1885.
[22] Drzal L, Madhukar M. Fibre-matrix adhesion and its relationship to composite mechanical properties. J Mater Sci 1993;28(3):569–610.
[23] Kelly A, Tyson W. Tensile properties of fibre-reinforced metals: Copper/tungsten and copper/molybdenum. J Mech Phys Solids 1965;13(6):329–50.
[24] Arbelaiz A, Cantero G, Fernández B, Mondragon I, Gañán P, Kenny J. Flax fiber surface modifications: Effects on fiber physico mechanical and flax/polypropylene interface properties. Polym Compos 2005;26(3):324–32.
[25] Wong S, Shanks R, Hodzic A. Effect of additives on the interfacial strength of poly(l-lactic acid) and poly(3-hydroxy butyric acid)-flax fibre composites. Compos Sci Technol 2007;67(11):2478–84.
[26] Spārniņš E, Nyström B, Andersons J. Interfacial shear strength of flax fibers in thermoset resins evaluated via tensile tests of UD composites. Int J Adhes Adhes 2012;36:39–43.
[27] Zafeiropoulos N, Baillie C, Hodgkinson J. Engineering and characterisation of the interface in flax fibre/polypropylene composite materials. Part II. The effect of surface treatments on the interface. Composites A 2002;33(9):1185–90.

[28] Huber T, Müssig J. Fibre matrix adhesion of natural fibres cotton, flax and hemp in polymeric matrices analyzed with the single fibre fragmentation test. Compos Interfaces 2008;15(2–3):335–49.
[29] Seghini M, Touchard F, Sarasini F, Chocinski-Arnault L, Mellier D, Tirillò J. Interfacial adhesion assessment in flax/epoxy and in flax/vinylester composites by single yarn fragmentation test: Correlation with micro-CT analysis. Composites A 2018;113:66–75.
[30] Joffe R, Andersons J, Wallström L. Interfacial shear strength of flax fiber/thermoset polymers estimated by fiber fragmentation tests. J Mater Sci 2005;40(9):2721–2.
[31] Khalil H, Ismail H, Rozman H, Ahmad M. The effect of acetylation on interfacial shear strength between plant fibres and various matrices. Eur Polym J 2001;37(5):1037–45.
[32] Baley C, Busnel F, Grohens Y, Sire O. Influence of chemical treatments on surface properties and adhesion of flax fibre–polyester resin. Composites A 2006;37(10):1626–37.
[33] Gaur U, Miller B. Microbond method for determination of the shear strength of a fiber/resin interface: Evaluation of experimental parameters. Compos Sci Technol 1989;34(1):35–51.
[34] Denissen W, Winne JM, Du Prez FE. Vitrimers: permanent organic networks with glass-like fluidity. Chem Sci 2016;7:30–8.
[35] Van Zee NJ, Nicolaÿ R. Vitrimers: Permanently crosslinked polymers with dynamic network topology. Prog Polym Sci 2020;104:101233.
[36] Zheng J, Png ZM, Ng SH, Tham GX, Ye E, Goh SS, Loh XJ, Li Z. Vitrimers: Current research trends and their emerging applications. Mater Today 2021;51:586–625.
[37] Lucherelli MA, Duval A, Avérous L. Biobased vitrimers: Towards sustainable and adaptable performing polymer materials. Prog Polym Sci 2022;127:101515.
[38] Ruiz de Luzuriaga A, Martin R, Markaide N, Rekondo A, Cabañero G, Rodríguez J, Odriozola I. Epoxy resin with exchangeable disulfide crosslinks to obtain reprocessable, repairable and recyclable fiber-reinforced thermoset composites. Mater Horiz 2016;3:241–7.
[39] Taynton P, Ni H, Zhu C, Yu K, Loob S, Jin Y, Qi HJ, Zhang W. Repairable woven carbon fiber composites with full recyclability enabled by malleable polyimine networks. Adv Mater 2016;28(15):2904–9.
[40] Directive E, et al. Directive 2008/98/EC of the European Parliament and of the Council of 19 November 2008 on waste and repealing certain Directives. Off J Eur Union L 2008;312(3).
[41] Arkema website. Elium® resins for composites. 2022, URL: https://www.arkema.com/global/en/products/product-finder/product-range/incubator/elium_resins, Accessed: 2022-03-30.
[42] Europa Eu website. Understanding REACH. 2022, URL: https://echa.europa.eu/regulations/reach/understanding-reach, Accessed: 2022-03-30.
[43] Bitrez website. Furacure (PFA). 2022, URL: https://www.bitrez.com/products/furacure-pfa/, Accessed: 2022-03-30.
[44] Montarnal D, Capelot M, Tournilhac F, Leibler L. Silica-like malleable materials from permanent organic networks. Science 2011;334(6058):965–8.
[45] Mallinda website. VITRIMAX™ product: the technology. 2022, URL: https://mallinda.com/product/, Accessed: 2022-03-30.
[46] Taynton P, Yu K, Shoemaker RK, Jin Y, Qi HJ, Zhang W. Heat- or water-driven malleability in a highly recyclable covalent network polymer. Adv Mater 2014;26(23):3938–42.
[47] Eichhorn SJ, Baillie CA, Zafeiropoulos N, Mwaikambo LY, Ansell MP, Dufresne A, Entwistle KM, Herrera-Franco PJ, Escamilla GC, Groom L, Hughes M, Hill C, Rials TG, Wild PM. Review: Current international research into cellulosic fibres and composites. J Mater Sci 2001;36(9):2107–31.
[48] Pitkethly M, Favre J, Gaur U, Jakubowski J, Mudrich S, Caldwell D, Drzal L, Nardin M, Wagner H, Landro LD, Hampe A, Armistead J, Desaeger M, Verpoest I. A round-robin programme on interfacial test methods. Compos Sci Technol 1993;48(1):205–14.
[49] Madhukar MS, Drzal LT. Fiber-matrix adhesion and its effect on composite mechanical properties: II. Longitudinal (0) and transverse (90) tensile and flexure behavior of graphite/epoxy composites. J Compos Mater 1991;25(8):958–91.
[50] Petersen R. Discontinuous fiber-reinforced composites above critical length. J Dent Res 2005;84(4):365–70.
[51] Robinson I, Robinson J. The effect of fibre aspect ratio on the stiffness of discontinuous fibre-reinforced composites. Composites 1994;25(7):499–503, Third International Conference on Interfacial Phenomena in Composite Materials.
[52] Dhers S, Vantomme G, Avérous L. A fully bio-based polyimine vitrimer derived from fructose. Green Chem 2019;21:1596–601.
[53] ASTM website. Standard test method for tensile properties of polymer matrix composite materials. Standard, West Conshohocken, PA: ASTM International; 2016, http://dx.doi.org/10.1520/D3039_D3039M-17.